results demonstrate that this limitation can be circumvented by operating below the length scale determined by the electron mean free path.

## REFERENCES AND NOTES


1. M. Lundstrom, *Science* **299**, 210–211 (2003).
2. B. Weber *et al*., *Science* **335**, 64–67 (2012).
3. Q. Xu, B. Schmidt, S. Pradhan, M. Lipson, *Nature* **435**, 325–327 (2005).
4. L. Novotny, B. Hecht, *Principles of Nano-optics* (Cambridge Univ. Press, Cambridge, 2012).
5. A. L. Falk *et al*., *Nat. Phys.* **5**, 475–479 (2009).
6. C. Henkel, S. Pötting, M. Wilkens, *Appl. Phys. B* **69**, 379–387 (1999).
7. Y. J. Lin, I. Teper, C. Chin, V. Vuletić, *Phys. Rev. Lett.* **92**, 050404 (2004).
8. M. P. A. Jones, C. J. Vale, D. Sahagun, B. V. Hall, E. A. Hinds, *Phys. Rev. Lett.* **91**, 080401 (2003).
9. D. Harber, J. McGuirk, J. Obrecht, E. Cornell, *J. Low Temp. Phys.* **133**, 229–238 (2003).
10. M. Brownnutt, M. Kumph, P. Rabl, R. Blatt, http://arxiv.org/abs/1409.6572 (2014).
11. L. S. Langsjoen, A. Poudel, M. G. Vavilov, R. Joynt, *Phys. Rev. A* **86**, 010301 (2012).
12. C. Beenakker, H. van Houten, *Solid State Phys.* **44**, 1–228 (1991).
13. S. Datta, *Electronic Transport in Mesoscopic Systems* (Cambridge Univ. Press, Cambridge, 1997).
14. A. C. Bleszynski-Jayich *et al*., *Science* **326**, 272–275 (2009).
15. H. Bluhm, N. C. Koshnick, J. A. Bert, M. E. Huber, K. A. Moler, *Phys. Rev. Lett.* **102**, 136802 (2009).
16. D. Rothfuß, A. Reiser, A. Fleischmann, C. Enss, *Appl. Phys. Lett.* **103**, 052605 (2013).
17. L. Childress *et al*., *Science* **314**, 281–285 (2006).
18. J. R. Maze *et al*., *Nature* **455**, 644–647 (2008).
19. G. Balasubramanian *et al*., *Nature* **455**, 648–651 (2008).
20. J. P. Tetienne *et al*., *Science* **344**, 1366–1369 (2014).
21. E. Schäfer-Nolte, L. Schlipf, M. Ternes, F. Reinhard, K. Kern, J. Wrachtrup, http://arxiv.org/abs/1406.0362 (2014).
22. M. Pelliccione, B. A. Myers, L. Pascal, A. Das, A. C. Bleszynski Jayich, http://arxiv.org/abs/1409.2422 (2014).
23. Materials and methods are available as supporting material on *Science* Online.
24. T. H. Taminiau, J. Cramer, T. van der Sar, V. V. Dobrovitski, R. Hanson, *Nat. Nanotechnol.* **9**, 171–176 (2014).
25. A. A. Baski, H. Fuchs, *Surf. Sci.* **313**, 275–288 (1994).
26. J. H. Park *et al*., *Adv. Mater.* **24**, 3988–3992 (2012).
27. G. W. Ford, W. Weber, *Phys. Rep.* **113**, 195–287 (1984).
28. N. W. Ashcroft, N. D. Mermin, *Solid State Physics* (Holt, Rinehart and Winston, New York, 1976).
29. P. Maher *et al*., *Science* **345**, 61–64 (2014).
30. L. Faoro, L. B. Ioffe, *Phys. Rev. Lett.* **100**, 227005 (2008).
31. S. M. Anton *et al*., *Phys. Rev. Lett.* **110**, 147002 (2013).


## ACKNOWLEDGMENTS

We thank E. Demler, A. Bleszynski Jayich, B. Myers, A. Yacoby, M. Vavilov, R. Joynt, A. Poudel, and L. Langsjoen for helpful discussions and insightful comments. Financial support was provided by the Center for Ultracold Atoms, the National Science Foundation (NSF), the Defense Advanced Research Projects Agency Quantum-Assisted Sensing and Readout program, the Air Force Office of Scientific Research Multidisciplinary University Research Initiative, and the Gordon and Betty Moore Foundation. S.K. and A.S. acknowledge financial support from the National Defense Science and Engineering Graduate fellowship, V.E.M. from the Society of Fellows of Harvard University, and S.K. from the NSF Graduate Research Fellowship. All fabrication and metrology were performed at the Center for Nanoscale Systems (CNS), a member of the National Nanotechnology Infrastructure Network, which is supported by the NSF under award no. ECS-0335765. The CNS is part of Harvard University.

## SUPPLEMENTARY MATERIALS

www.sciencemag.org/content/347/6226/1129/suppl/DC1
Materials and Methods
Figs. S1 to S7
Tables S1 to S3
References (*32*–*34*)

4 December 2014; accepted 16 January 2015
Published online 29 January 2015;
10.1126/science.aaa4298

REPELLENT MATERIALS

# Robust self-cleaning surfaces that function when exposed to either air or oil

**Yao Lu,[1] Sanjayan Sathasivam,[1] Jinlong Song,[2] Colin R. Crick,[3] Claire J. Carmalt,[1] Ivan P. Parkin[1]***

**Superhydrophobic self-cleaning surfaces are based on the surface micro/nanomorphologies; however, such surfaces are mechanically weak and stop functioning when exposed to oil. We have created an ethanolic suspension of perfluorosilane-coated titanium dioxide nanoparticles that forms a paint that can be sprayed, dipped, or extruded onto both hard and soft materials to create a self-cleaning surface that functions even upon emersion in oil. Commercial adhesives were used to bond the paint to various substrates and promote robustness. These surfaces maintained their water repellency after finger-wipe, knife-scratch, and even 40 abrasion cycles with sandpaper. The formulations developed can be used on clothes, paper, glass, and steel for a myriad of self-cleaning applications.**

Artificial self-cleaning surfaces work through extreme water repellence (superhydrophobicity) so that water forms near spherical shapes that roll on the surface; the rolling motion picks up and removes dirt, viruses, and bacteria (*1*–*3*). To achieve near spherical water droplets, the surfaces must be highly textured (rough) combined with extremely low water affinity (waxy) (*4*, *5*). The big drawback of these artificial surfaces is that they are readily abraded (*6*–*8*), sometimes with little more than brushing with a tissue, and readily contaminated by oil (*9*–*11*). We report here a facile method for making superhydrophobic surfaces from both soft (cotton or paper) and hard (metal or glass) materials. The process uses dual-scale nanoparticles of titanium dioxide ($TiO_2$) that are coated with perfluorooctyltriethoxysilane. We created an ethanol-based suspension that can be sprayed, dipped, or painted onto surfaces to create a resilient water-repellent surface. By combining the paint and adhesives, we created a superhydrophobic surface that showed resilience and maintained its performance after various types of damage, including finger-wipe, knife-scratch, and multiple abrasion cycles with sandpaper. This method can also be used for components that require self-cleaning and lubricating such as bearings and gears, to which superamphiphobic (repels oil and water) surfaces (*9*–*11*) are not applicable.

A paint was created by mixing two different size ranges of $TiO_2$ nanoparticles (~60 to 200 nm and ~21 nm) in an ethanol solution containing perfluorooctyltriethoxysilane (*12*). Scanning electron microscopy (SEM) and transmission electron microscopy (TEM) of the constituent particles of the paint (Fig. 1A) show the dual-scale nature of the $TiO_2$ nanoparticles. X-ray photoelectron spectroscopy (XPS) (Fig. 1B) showed that the titanium dioxide particles were coated with perfluorooctyltriethoxysilane.

We used many different coating methods to create the water-repellent surfaces, including an artist's spray-gun to coat hard substrates such as glass and steel, dip-coating for cotton wool, and a syringe (movie S1) to extrude the paint onto filter paper. After allowing the ethanol to evaporate for ~180 s at room temperature, the treated areas of the substrates supported water as near spherical droplets, whereas the untreated parts were readily wetted (it required ~30 min for the ethanol to fully evaporate from cotton wool and filter paper at room temperature) (fig. S1). We used x-ray diffraction (XRD) (Fig. 1C) to analyze the coatings on hard and soft substrates. The diffraction peaks show the expected patterns for nanoscaled $TiO_2$.

On a surface that shows water repellence, water droplets tend to bounce instead of wetting the surface (*13*, *14*). However, for soft substrates, extreme superhydrophobicity is required to achieve the bouncing phenomenon because the water droplets tend to be trapped onto the threads of the substrates (cotton wool) (*15*). Shown in fig. S2 are the water dropping tests on untreated glass, steel, cotton wool, and filter paper, which were readily wetted (the contact moment of the water droplets and the solid surfaces is defined as 0). Shown in Fig. 2 is the water bouncing process on dip-coated glass, steel, cotton wool, and filter paper surfaces. Water droplets completely leave the surface without wetting or even contaminating the surfaces (the water was dyed blue to aid visualization), indicating that the surfaces were superhydrophobic. In movie S2, we compare the water-affecting behavior between untreated and treated glass, steel, cotton wool, and filter paper, respectively. The effect of artificial rain on the treated surfaces is shown in movie S3; the drop sizes varied with random impact

[1]Department of Chemistry, University College London, 20 Gordon Street, London, WC1H 0AJ, UK. [2]Key Laboratory for Precision and Non-traditional Machining Technology of Ministry of Education, Dalian University of Technology, Dalian, 116024, People's Republic of China. [3]Department of Chemistry, Imperial College London, South Kensington Campus, London, SW7 2AZ, UK.
*Corresponding author. E-mail: i.p.parkin@ucl.ac.uk

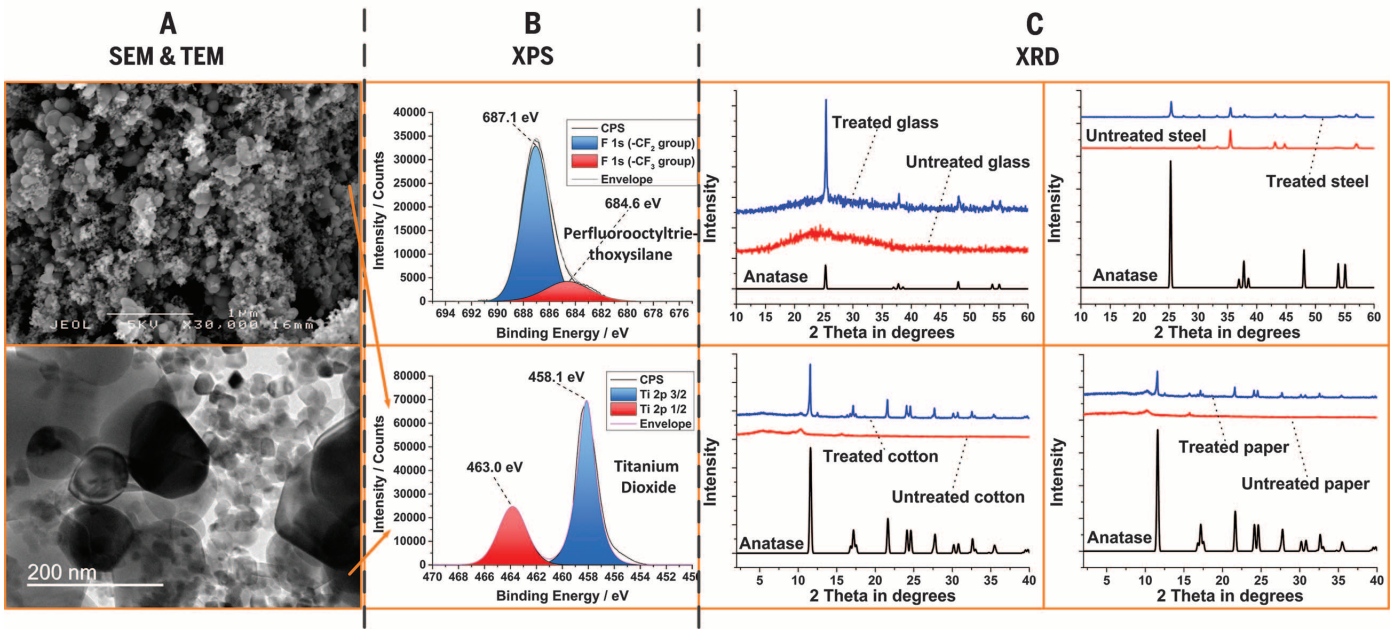


**Fig. 1. Paint characterizations.** (**A**) SEM (top) and TEM (bottom) of the constituent nanoparticles in the paint. Sizes varied from ~60 to 200 nm for the $TiO_2$ nanoparticles (Aldrich), whereas ~21 nm in size refers to P25. (**B**) XPS of the paint, where "F" refers to perfluorooctyltriethoxysilane and "Ti" refers to $TiO_2$. (**C**) XRD patterns of treated and untreated substrates compared with the respective standard patterns for $TiO_2$ anatase (the P25 particles had a small rutile component, as expected).

velocities, and the droplets could not wet the treated surfaces.

The paint had good self-cleaning properties when applied on various substrates, especially for soft porous materials, such as those used in making clothes and paper. The coated surfaces show water-proofing properties from the water-bouncing and artificial rain tests. Further tests on cotton wool and filter paper are shown in figs. S3 (the experimental scheme) and S4 (the experimental results). As shown in fig. S4, A and B, the dip-coated cotton wool inserted into the methylene blue–dyed water formed a negative meniscus on the solid-liquid-vapor interfaces because of hydrophobicity (*16*). The cotton wool was removed from the water and remained fully white with no trace of contamination by the dyed water (fig. S3). A dirt removal test when an artificial dust (MnO powder) was put on the spray-coated filter paper, which was then cleaned by pouring water, is shown in fig. S4, C and D. The untreated piece of filter paper (placed below) was wet and polluted by the dirt, whereas the treated piece stayed dry and clean (fig. S3). The self-cleaning tests on the dip-coated cotton wool and spray-coated filter paper are shown in movie S4; a time-lapsed video clip of water droplets (dyed blue) staying on the dip-coated cotton wool and syringe-coated filter paper for 10 min is shown in movie S5, and neither the cotton wool nor the filter paper had blue left after the droplets were removed. These tests indicate that the soft substrates (cotton and paper) gained the nonwetting and self-cleaning properties after treating with the paint. Dirt removal tests were also carried out on dip-coated glass and steel surfaces; as shown in fig. S4, E and F, the droplet took the dirt (MnO powder) away, and the surfaces were cleaned along the path of the water droplet movement. The self-cleaning property of dip-coated glass and steel surfaces is shown in movie S6 in a high-speed motion capture.

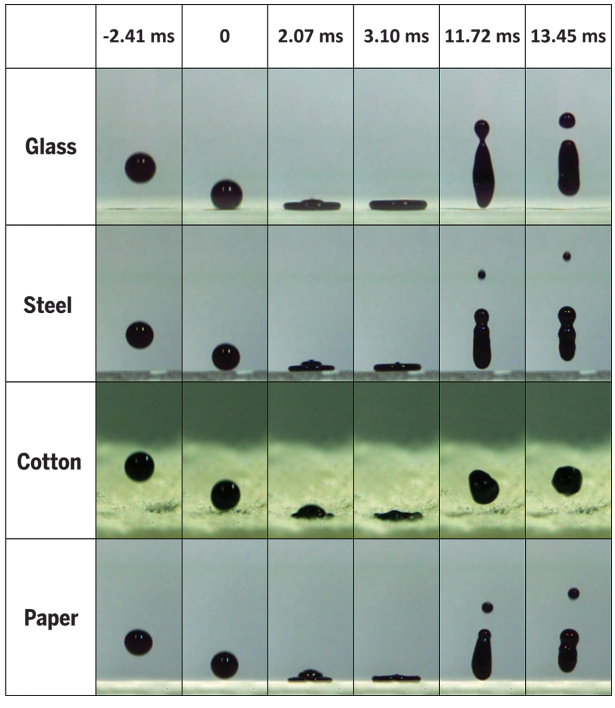


**Fig. 2. Time-lapse photographs of water droplets bouncing on the treated glass, steel, cotton wool, and filter paper surfaces.** Droplet sizes, ~6.3 ± 0.2 μL.

Very few reports have shown any self-cleaning tests in oil because superhydrophobic surfaces normally lose their water repellency when even partially contaminated by oil. This is because the surface tension of the oil is lower than that of water, resulting in the oil penetrating through the surfaces. Making superamphiphobic surfaces (that repel both water and oils) is an effective way to solve this problem (*9*, *10*, *17*). However, there are many instances that require both self-cleaning from water repellency and a smooth coating of oil, such as lubricating bearings and gears; under these conditions, superamphiphobic surfaces cannot be used because they will also repel lubricating oils.

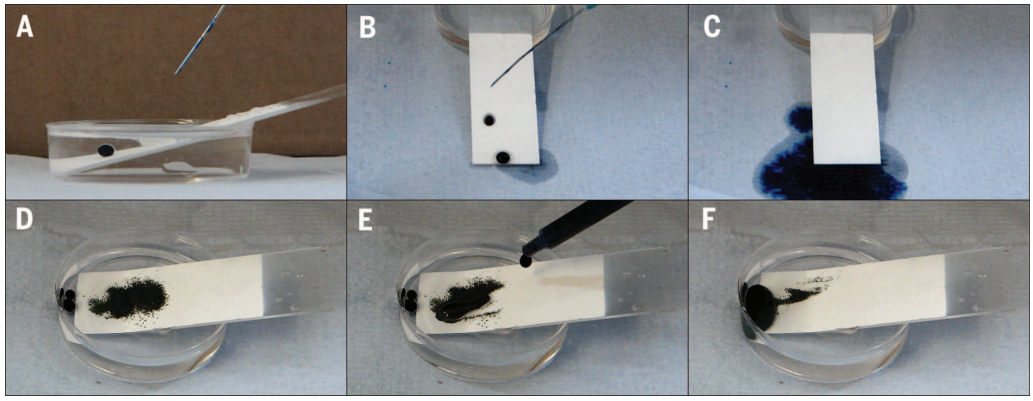


**Fig. 3. Self-cleaning tests after oil-contaminations.** (**A**) Water droplet was repelled by the treated surface when immersed in oil (hexadecane). (**B** and **C**) The treated surface retained its water-repellent property even after being contaminated by oil (**D** to **F**) The dirt removal test in oil-solid-vapor interfaces. Dirt was put partly in oil and air, the surface was contaminated by oil, water was dropped onto the surface, and this removed the dirt both in air and oil.

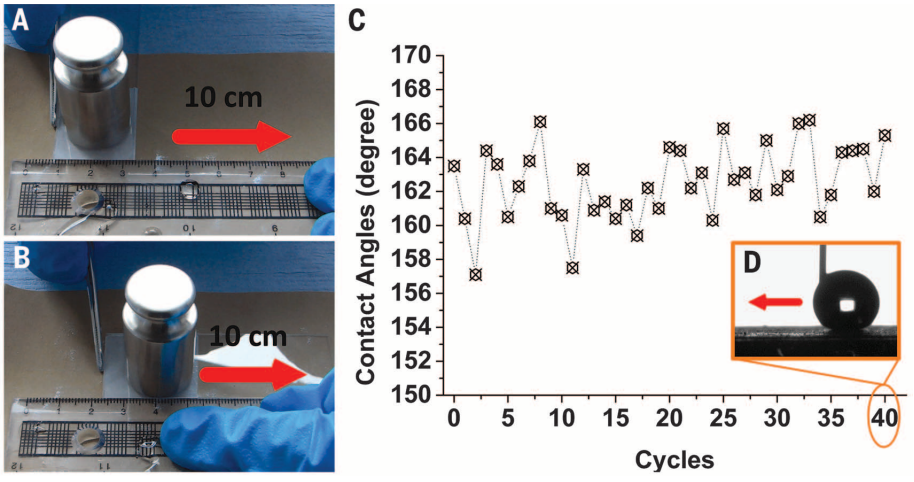


**Fig. 4. Sandpaper abrasion tests.** (**A** and **B**) One cycle of the sandpaper abrasion test. (**C**) Plot of mechanical abrasion cycles and water contact angles after each abrasion test. (**D**) Water droplet traveling test after 40th cycle abrasion.

The self-cleaning tests of the painted surfaces after oil (hexadecane) contamination and immersion are presented graphically in fig. S5. As shown in fig. S6, water droplets still formed "marbles" on the dip-coated surface when immersed in oil, rather than forming a two-layer system (fig. S5A), thus indicating that the surfaces will retain their self-cleaning properties after being immersed in oil. For example, on the untreated areas of a glass slide, water droplets spread and wet the surfaces. We show in movie S7 water dropped on the dip-coated and untreated surfaces immersed in oil. We show in Fig. 3A the side view of a water droplet that formed a sphere at the oil-solid interface without wetting a spray-coated surface; the droplet then rolled off from the surface. As shown in Fig. 3, B and C, the water droplets slipped off from the spray-coated surface that was contaminated by oil (hexadecane), indicating self-cleaning was retained even after oil-contamination (fig. S5B and movie S8). We show in Fig. 3, D to F, a dirt-removal test on the spray-coated surfaces both in oil and air. The treated surface was fully contaminated by oil and then partly inserted into oil; dirt (MnO powder) was also put partly in oil and air onto the surface. Water was dropped so as to remove the dirt both in air and oil (fig. S5C and movie S9). This was to test the dirt-removal properties of the oil-contaminated painted surface both in air and under oil. For further dirt-removal tests on oil-contaminated painted surfaces, we used soil, household dust, and cooking oil from actual conditions and repeated the experiments shown in fig. S5C. As shown in fig. S7, soil and dust were removed by water from the dip-coated surfaces immersed either in hexadecane or cooking oil.

When the treated surfaces were immersed in oil, the oil gradually penetrated into the surface, so the water droplets were supported by both oil and the surface structures and were still marble-shaped (fig. S6). In this condition, the self-cleaning behavior in oil is similar to that in air (*18*–*20*); thus, the treated surfaces retained the water-repellent and dirt-removal properties when immersed in oil (Fig. 3, D to F). In air, when the treated surfaces were contaminated by oil, the surface structures locked the oil as a lubricating fluid, and a slippery state was then achieved (*21*–*24*). Dirt was removed from the treated surfaces simply by passing water over the surface. For these reasons, the treated surfaces retained their self-cleaning properties when being contaminated by oil.

Low surface robustness is the main issue limiting the widespread application of superhydrophobic coatings because the surface roughness is usually at the micro- or nanoscale and is mechanically weak and readily abraded (*25*). This surface roughness is partially protected by soft substrates, such as cotton wool and filter paper, because of their inherent flexibility (*6*, *26*) and ability to reduce direct friction between the coating and the surface. However, on hard substrates such as glass, nanostructures are easily destroyed or removed. We developed a method to bond the self-cleaning coatings to the substrates by using adhesives so as to apply more sophisticated and robust adhesive techniques and overcome the weak inherent robustness of superhydrophobic surfaces. We show in fig. S8 the "paint + adhesive (double-sided tape/spray adhesive) + substrates" sample preparation methods (fig. S8, A and B) and the relevant robustness tests, including finger-wipe (fig. S8C), knife-scratch (fig. S8D), and sandpaper abrasion (fig. S8, E and F). We show in fig. S9 and movie S10 the finger-wipe tests that compare the untreated, paint-treated, and "paint + double-sided tape"–treated (PDT) glass and steel substrates, respectively. After the finger-wipe, the paint directly coated on substrates was removed, whereas the double-sided tape-bonded paint was still left on the substrates, and the surfaces retained superhydrophobicity. Although the inherent robustness of the paint is intrinsically as weak as most superhydrophobic surfaces, it is friendly to adhesives, from which the robustness was gained. A glass substrate was used as one example for further robustness tests with double-sided tapes (knife-scratch and sandpaper abrasion tests); as shown in movie S10, the glass bonded with double-sided tape, and the paint still kept dry and clean after the knife-scratch and then water drop. The sandpaper abrasion tests were carried out on the PDT glass. The PDT glass weighing 100 g was placed face-down to sandpaper (standard glass-paper, grit no. 240) and moved for 10 cm along the ruler (Fig. 4A); the sample was rotated by 90° (face to the sandpaper) and then moved for 10 cm along the ruler (Fig. 4B). This process is defined as one abrasion cycle (movie S11), which guarantees the surface is abraded longitudinally and transversely in each cycle even if it is moved in a single direction. The water contact angles after each abrasion cycle are shown in Fig. 4C, and it was observed that the static water contact angles were between 156° and 168°, indicating superhydrophobicity was not lost by mechanical abrasion.

In order to test whether this superhydrophobicity was kept after abrasion on the whole area but not merely on some points (contact angle measuring points), water droplet was guided by a needle to travel on the PDT glass surface after the 11th, 20th, 30th, and 40th cycle's abrasion, respectively (movie S12). The water droplet traveling after the 40th cycle is shown in Fig. 4D.

To enlarge the application scale and broaden the types of substrates, the spray adhesive [EVO-STIK (Bostik, UK)] was also used to bond glass, steel, cotton wool, and filter paper substrates with the superhydrophobic paint. We show in fig. S10 and movie S13 the finger-wipe tests on untreated, paint-treated, and "paint + spray adhesive"–treated (PSAT) substrates, respectively. On hard substrates (glass and steel), PSAT surfaces retained water proofing, whereas the paint was just removed when directly applied; the case is different on soft substrates (cotton and paper), on which paint was protected by their porous structures, resulting in both paint-treated and PSAT cotton and paper being superhydrophobic after the finger-wipe. However, in a more powerful test (sandpaper abrasion of cotton), this "protection" is limited (fig. S11). As shown in fig. S12 and movie S14, the sandpaper abrasion tests on PSAT substrates and both hard and soft substrates became robust after the PSAT treatment. As shown in fig. S13 and movie S15, the PSAT substrates retained water repellency after knife-scratch tests. After different damages, the PSAT materials still remained superhydrophobic, indicating that this method could efficiently enhance the robustness of superhydrophobic surfaces on different substrates; it is believed that the idea of "superhydrophobic paint + adhesives" can be simply, flexibly, and robustly used in large-scale industrial applications.

The superhydrophobic surfaces show that a robust resistance to oil contamination and ease of applicability can be achieved by implementing straightforward coating methods such as spraying, dip-coating, or even simply extrusion from a syringe. The flexibility of the "paint + adhesives" combination enables both hard and soft substrates to become robustly superhydrophobic and self-cleaning. The surfaces can be readily implemented in harsh and oily environments where robustness is required.

## REFERENCES AND NOTES


1. W. Barthlott, C. Neinhuis, *Planta* **202**, 1–8 (1997).
2. R. Blossey, *Nat. Mater.* **2**, 301–306 (2003).
3. I. P. Parkin, R. G. Palgrave, *J. Mater. Chem.* **15**, 1689 (2005).
4. T. Onda, S. Shibuichi, N. Satoh, K. Tsujii, *Langmuir* **12**, 2125–2127 (1996).
5. L. Feng *et al.*, *Adv. Mater.* **14**, 1857–1860 (2002).
6. J. Zimmermann, F. A. Reifler, G. Fortunato, L. C. Gerhardt, S. Seeger, *Adv. Funct. Mater.* **18**, 3662–3669 (2008).
7. X. Zhu *et al.*, *J. Mater. Chem.* **21**, 15793 (2011).
8. Q. Zhu *et al.*, *J. Mater. Chem. A* **1**, 5386 (2013).
9. A. Tuteja *et al.*, *Science* **318**, 1618–1622 (2007).
10. X. Deng, L. Mammen, H. J. Butt, D. Vollmer, *Science* **335**, 67–70 (2012).
11. Y. Lu *et al.*, *ACS Sustainable Chem. Eng.* **1**, 102 (2013).
12. Materials and methods are available as supplementary materials on *Science* Online.
13. D. Richard, C. Clanet, D. Quéré, *Nature* **417**, 811 (2002).
14. J. C. Bird, R. Dhiman, H. M. Kwon, K. K. Varanasi, *Nature* **503**, 385–388 (2013).
15. Y. Lu *et al.*, *J. Mater. Chem. A* **2**, 12177 (2014).
16. D. Vella, L. Mahadevan, *Am. J. Phys.* **73**, 817 (2005).
17. A. Tuteja, W. Choi, J. M. Mabry, G. H. McKinley, R. E. Cohen, *Proc. Natl. Acad. Sci. U.S.A.* **105**, 18200–18205 (2008).
18. A. Nakajima *et al.*, *Langmuir* **16**, 7044–7047 (2000).
19. R. Fürstner, W. Barthlott, C. Neinhuis, P. Walzel, *Langmuir* **21**, 956–961 (2005).
20. B. Bhushan, Y. C. Jung, K. Koch, *Langmuir* **25**, 3240–3248 (2009).
21. T. S. Wong *et al.*, *Nature* **477**, 443–447 (2011).
22. M. Nosonovsky, *Nature* **477**, 412–413 (2011).
23. A. Grinthal, J. Aizenberg, *Chem. Mater.* **26**, 698–708 (2014).
24. D. C. Leslie *et al.*, *Nat. Biotechnol.* **32**, 1134–1140 (2014).
25. M. Im, H. Im, J. Lee, J. Yoon, Y. Choi, *Soft Matter* **6**, 1401 (2010).
26. B. Wang *et al.*, *ACS Appl. Mater. Interfaces* **5**, 1827–1839 (2013).



## ACKNOWLEDGMENTS

We thank M. Vickers and S. Firth for XRD and TEM characterizations. Thanks to C. E. Knapp and D. S. Bhachu for ordering chemicals and the help with some experiments.


## SUPPLEMENTARY MATERIALS

www.sciencemag.org/content/347/6226/1132/suppl/DC1
Materials and Methods
Supplementary Text
Figs. S1 to S13
References (*27*, *28*)
Movies S1 to S15

16 October 2014; accepted 30 January 2015
10.1126/science.aaa0946

PROTEIN IMAGING

# Single-protein spin resonance spectroscopy under ambient conditions

**Fazhan Shi,[1,2,3]* Qi Zhang,[1,2]* Pengfei Wang,[1,2,3]* Hongbin Sun,[4] Jiarong Wang,[4] Xing Rong,[1,2,3] Ming Chen,[1,2] Chenyong Ju,[1,2,3] Friedemann Reinhard,[5]† Hongwei Chen,[4] Jörg Wrachtrup,[5] Junfeng Wang,[4] Jiangfeng Du[1,2,3]‡**

**Magnetic resonance is essential in revealing the structure and dynamics of biomolecules. However, measuring the magnetic resonance spectrum of single biomolecules has remained an elusive goal. We demonstrate the detection of the electron spin resonance signal from a single spin-labeled protein under ambient conditions. As a sensor, we use a single nitrogen vacancy center in bulk diamond in close proximity to the protein. We measure the orientation of the spin label at the protein and detect the impact of protein motion on the spin label dynamics. In addition, we coherently drive the spin at the protein, which is a prerequisite for studies involving polarization of nuclear spins of the protein or detailed structure analysis of the protein itself.**

Observing the structure and dynamics of single molecules is a long-sought goal that has inspired technical developments in a wide range of disciplines (*1*–*4*). As one of the most important techniques, electron spin resonance (ESR) finds broad application for studying basic molecular mechanisms in biology and chemistry (*5*). Most proteins, however, are nonparamagnetic and thus cannot be accessed by the technique. Labeling biomolecules with a small spin-bearing moiety, such as nitroxide spin labels, enables ESR to acquire a broad range of structural and dynamical information. However, current methods need $10^{10}$ uniform molecules to accumulate a large enough signal-to-noise ratio. This substantially complicates efforts to compile structural and dynamical information. New methods that have tried to push the sensitivity of magnetic resonance to the single-spin level all require either a dedicated environment (*6*, *7*) or conducting surfaces and tips (*8*).

A sensor that could accomplish single-protein detection under ambient conditions is a recently developed atomic-sized magnetic field sensor based on the nitrogen vacancy (NV) defect center in diamond (*9*–*11*). Because of its long coherence times (*12*, *13*), the NV sensor can detect a single electron spin over a distance of 30 nm under ambient conditions. As proof-of-principle demonstrations, single electron spins inside diamond or on diamond surfaces have been sensed (*14*–*16*). Despite previous efforts, single-biomolecule detection and spectroscopy have not been attained. Here, we report an electron spin resonance study on a single protein, which allows us to extract the structural and dynamical properties from spectral analysis.

As the experimental sample, we chose MAD2 (mitotic arrest deficient-2), an essential spindle

[1]Hefei National Laboratory for Physical Sciences at the Microscale and Department of Modern Physics, University of Science and Technology of China (USTC), Hefei 230026, China. [2]Joint Laboratory of Quantum Biophysics, USTC Institute of Biophysics and Chinese Academy of Sciences. [3]Synergetic Innovation Center of Quantum Information and Quantum Physics, USTC, Hefei 230026, China. [4]High Magnetic Field Laboratory, Chinese Academy of Sciences, Hefei 230000, China. [5]3rd Physics and Integrated Quantum Science and Technology (IQST), University of Stuttgart, 70569 Stuttgart, Germany.
*These authors contributed equally to this work. †Present address: Walter Schottky Institut, E24, Technische Universität München, 85748 Garching, Germany. ‡Corresponding author. E-mail: djf@ustc.edu.cn

# Robust self-cleaning surfaces that function when exposed to either air or oil

Yao Lu *et al.*

*Science* **347**, 1132 (2015);
DOI: 10.1126/science.aaa0946